RESEARCH REPORT RR-007

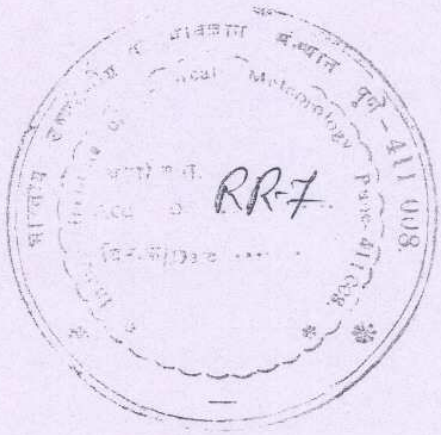

A THEORETICAL STUDY OF MOUNTAIN WAVES IN ASSAM

by

U. S. De

INDIAN INSTITUTE OF TROPICAL METEOROLOGY

Ramdurg House
Ganeshkhind Road,
Poona-5, India

February 1973

A Theoretical study of mountain waves in Assam

by

U. S. De

Indian Institute of Tropical Meteorology, Poona-5.

ABSTRACT

The paper presents the results of an investigation on mountain waves for the Assam hills and its neighbouring region. Computations of vertical velocity were made using a two dimensional linearised model by analytical and numerical methods for several situations in the winter season when the occurrence of lee waves in the region are seen on weather satellite cloud observations. Important aspects of the SW flow pattern have been discussed.

1. Introduction

It is well known that when air flows over an obstacle, waves are formed to the lee of the barrier, under suitable conditions of thermal stratification and wind shear. Scorer (1949), using a realistic distribution of wind and temperature in the atmosphere, derived solutions of the equation

$$\frac{\partial^2 \psi}{\partial x^2} + \frac{\partial^2 \psi}{\partial z^2} + l^2 \psi = 0 , \qquad \ldots \quad (1.1)$$

where ψ is a perturbation in the stream function on account of the barrier and

$$l^2 = \frac{g\beta}{U^2} - \frac{1}{U}\frac{d^2U}{dz^2} , \quad \beta = \frac{1}{\theta}\frac{d\theta}{dz} \qquad \ldots (1.2)$$

Here, θ is the undisturbed potential temperature and U is undisturbed wind velocity. θ and U are functions of z only, and g is the

... 2

acceleration due to gravity. The x-axis points eastwards while Z is the vertical axis reckoned to be positive upwards. Scorer established that for lee waves to form, l^2 should decrease with height.

Solutions to the above equation were obtained by assuming two layers in the atmosphere with different values of l^2. Sawyer (1960) studied the problem numerically by integrating the wave equation used in Scorer's problem. Palm (1958), Palm and Foldvik (1960), Foldvik and Palm (1957, 1959) and Doos (1962, 1961, 1958) used an exponential representation for the function l^2 to denote its variation with height and obtained solutions in terms of Bessel functions. Sarker (1965), using a similar method, obtained solutions for the vertical perturbation velocity for the Western Ghats in India. In his subsequent work, he numerically integrated the equations used in his earlier study to compute orographic rainfall during the monsoon season for the Western Ghats. Das (1964) studied the effect of Himalayas on large scale flow patterns in the westerlies as a three dimensional problem.

In this paper we solve the two dimensional linearised problem by analytical and numerical methods with particular reference to the Assam hills.

2. Mountain wave equation

We consider a two dimensional system of axes with x axis pointing eastwards and the Z axis directed vertically upwards. Let the perturbation variables be denoted by u, o, w, ρ and T while the corresponding undisturbed values of the same variables are $\bar{U}$, o, o, $\bar{\rho}$ and $\bar{T}$,

... 3

where $\bar{U}$, $\bar{\varrho}$ and $\bar{T}$ are functions of Z only. By a process of elimination (Palm and Foldvik (1960)), we obtain the following equation for the vertical perturbation velocity,

$$\frac{\partial^2 w}{\partial x^2} + \frac{\partial^2 w}{\partial Z^2} - \left(\frac{g - R\nu}{2\,R\bar{T}} \right) \frac{\partial w}{\partial Z} + \left| \frac{g\,(\nu^* - \nu)}{\bar{U}^2\,\bar{T}} - \frac{1}{\bar{U}} \frac{d^2\bar{U}}{dZ^2} \right.$$

$$\left. + \left\{ \frac{(\nu^* - \nu)}{\bar{T}} - \frac{g}{\chi R\bar{T}} \right\} \frac{1}{\bar{U}} \frac{d\bar{U}}{dZ} - \frac{2}{\chi R\bar{T}} \frac{d\bar{U}}{dZ} \right| w = 0 \qquad \ldots (2.1)$$

where

ν^* is the dry adiabatic lapse rate

ν is the actual lapse rate

$\chi = \dfrac{g}{g - R\nu}$

and R is the universal gas constant.

The dependent variable W represents the vertical component of the perturbation velocity.

We introduce a new variable W_1 given by,

$$W = W_1 \exp\left(\frac{g - R\nu}{2\,R\bar{T}}\, Z \right) \qquad \ldots (2.2)$$

The small variation of $\left(\dfrac{g - R\nu}{2\,R\bar{T}} \right)$ with height is disregarded when we differentiate (2.2) with respect to Z. Equation (2.1) is thus transformed to

$$\frac{\partial^2 W_1}{\partial x^2} + \frac{\partial^2 W_1}{\partial Z^2} + f(Z)\, W_1 = 0 \qquad \ldots (2.3)$$

... 4

where,

$$f(Z) = \frac{g\,(\nu^* - \nu)}{\bar{U}^2\,\bar{T}} - \frac{1}{\bar{U}}\frac{d^2\bar{U}}{dZ^2} + \frac{1}{\bar{U}}\frac{d\bar{U}}{dZ}\left(\frac{(\nu^* - \nu)}{\bar{T}} - \frac{g}{xR\bar{T}}\right) - \frac{2}{xR\bar{T}}\left(\frac{d\bar{U}}{dZ}\right)^2 - \left(\frac{g - R\nu}{2R\bar{T}}\right)^2 \quad \ldots \quad (2.4)$$

In this paper, (2.3) was solved with suitable boundary conditions by analytical and numerical methods. We discuss the method of solutions, and the results obtained for the Assam hills.

3. The mountain profile

The Assam hills run in a north-south direction from the Naga hills to the north to the Lushai hills to the south, with an average elevation varying between 0.5 to 1 km. We have considered a section of the hills along the latitude belt 24-25°N from 93°E to 95°E. This area encloses the Manipur hills. The average topography of the area may be represented by combining two ridges of different heights separated by a distance. This is shown in Fig. 1. We have then for the mountain profile the following expression,

$$\zeta\,(x) = \frac{a^2 b_1}{a^2 + x^2} + \frac{a^2\,b_2}{a^2 + (x - d)^2} \quad \ldots \quad (3.1)$$

where b_1 and b_2 are heights of two ridges, a is the half-width, and d is the distance seperating the two ridges.

4. Analytical solutions

To obtain an analytical solution of equation (2.3) we need to specity the function f(Z). For a stable stratification f(Z) decreases

... 5

with height and can be well represented by the exponential function,

$$f(Z) = f_o \, e^{-\lambda Z} \qquad \ldots \qquad (4.1)$$

where f_o and λ are constants. We first assume the ground profile to be sinusoidal, and then generalise the solution by Fourier integrals for an arbitrary profile.

Let,

$$W_1 = W \, e^{ikx} \qquad \ldots \qquad (4.2)$$

Substitution of (4.1) and (4.2) in (2.3) leads to,

$$\eta^2 \frac{d^2 W}{d \eta^2} + \eta \frac{dW}{d\eta} + \left(\eta^2 - \frac{4K^2}{\lambda^2} \right) W = 0 \qquad \ldots \qquad (4.3)$$

where

$$\eta = \beta \, e^{-\frac{\lambda Z}{2}}$$

$$\beta = \frac{2 (f_o)^{\frac{1}{2}}}{\lambda} \qquad \ldots \qquad (4.4)$$

General solution of (4.3) is,

$$W = A J_m (\eta) + B Y_m (\eta)$$

$$= A J_m (\beta \, e^{-\lambda Z/2}) + B \, Y_m (\beta \, e^{-\lambda Z/2}) \qquad (4.5)$$

where $m = \frac{2K}{\lambda}$, and J_m and Y_m are Bessel functions of first and second kind of order m and argument η .

Both m and η are real.

The boundary conditions to determine A and B are :-

... 6

(A) Upper boundary

$$W(x,Z) \to 0 \qquad \text{as} \qquad Z \to \infty$$

This implies that the energy remains finite at great heights. As the second solution in (4.5) becomes infinitely large at great heights, we put $B = 0$.

Consequently,

$$W = A \exp(ikx) \exp\left(\frac{g - R\nu}{2R\bar{T}} Z\right) \times J_m\left(\beta e^{\frac{-\lambda Z}{2}}\right) \qquad \ldots (4.6)$$

(B) The lower boundary

At the lower boundary we consider the flow to be tangential to the surface. For the profile given by (3.1) this implies,

$$W(x, \zeta) = \bar{U}(\zeta) \frac{\partial}{\partial x} \zeta(x) \qquad \ldots (4.7)$$

Hence, the linearised lower boundary condition for a ridge of the form,

$$\xi(x) = \int_0^\infty e^{-ak} ab \cos kx \, dk$$

is,

$$W(x, 0) = \bar{U}(0) \frac{\partial}{\partial x} \int_0^\infty e^{-ak} ab \cos kx \, dk \qquad \ldots (4.8)$$

Consequently, the solution satisfying the lower boundary condition is

$$W(x, Z) = \bar{U}(0) \exp\left(\frac{g - R\nu}{2R\bar{T}} Z\right) \frac{\partial}{\partial x} \int_0^\infty \frac{e^{-ak} ab \cos kx \, J_m(\beta e^{-\lambda Z/2})}{J_m(\beta)} dk$$

... 7

The integral in (4.9) is an improper integral as $J_m(\beta)$ may vanish for real values of k. The roots of the equations $J_m(\beta) = 0$ which represent the singularities of the integrand, determine the lee waves. We shall, evaluate the Cauchy principal value of this integral. Accordingly, we integrate (4.9) along the contour shown in Fig.2.

For this purpose we put,

$$\int_C e^{-ak}\, ab \cos kx \times \frac{J_m(\beta\, e^{-\lambda Z/2})}{J_m(\beta)}\, dk$$

$$= \mathrm{Re} \int_C e^{-ak}\, \frac{e^{ikx}\, ab\, J_m(\beta\, e^{-\lambda Z/2})}{J_m(\beta)}\, dk \quad \text{for } x > 0$$

$$= \mathrm{Re} \int_C e^{-ak}\, \frac{e^{-ikx}\, ab\, J_m(\beta\, e^{-\lambda Z/2})}{J_m(\beta)}\, dk \quad \text{for } x < 0 \qquad \ldots (4.10)$$

where C is the path of integration shown in Fig.2, and Re indicates the real part of the integral. The solution is not unique when the motion is stationary and free waves exist. To make the solution unique, we adopt the method due to Kelvin (1886), that is, we add free waves that will nullify the waves on the upstream side of the barrier extending upto infinity. Performing the integration, and allowing the radii of the indentations to tend to zero and the radius of the arc to tend to infinity, we find,

$$W(x, Z) = W_p + W_r$$

where W_r represents the wave part, i.e., the contribution to the integral

... 8

due to a singularity or singularities and W_p is the contribution along the imaginary axis. We have, for the region

$x \geq 0$,

$$W_p = \bar{U}(0) \exp\left(\frac{g - R\nu}{2R\bar{T}} Z\right) \times I \int_0^{\infty} e^{-iak} \frac{e^{-kx} abk\, J_{im}(\beta e^{-\lambda Z/2})}{J_{im}(\beta)} dk \quad \ldots (4.11)$$

$$W_r = -\bar{U}(0) \exp\left(\frac{g - R\nu}{2R\bar{T}} Z\right) \times 2\pi \sum_{n=1}^{N} abk_n e^{-akn} \frac{\cos Knx\, J_{mn}(\beta e^{-\lambda Z/2})}{\frac{d}{dk} J_{mn}(\beta)}$$

While for $x < 0$,

$$W_p = \bar{U}(0) \exp\left(\frac{g - R\nu}{2R\bar{T}} Z\right) \times I \int_0^{\infty} e^{-iak} \frac{e^{kx} abk\, J_{im}(\beta e^{-\lambda Z/2})}{J_{im}(\beta)} dk \quad \ldots (4.12)$$

$$W_r = 0$$

where, m_n's represent the zeros of $J_m(\beta)$ and Km_n's the corresponding wave numbers. In evaluating W_p we consider the integral along the imaginary axis, and as m is a function of K, $J_m(\beta)$ and $J_m(\beta e^{-\lambda Z/2})$ are expressed as $J_{im}(\beta)$ and $J_{im}(\beta e^{-\lambda Z/2})$. By I we represent the imaginary part of an integral. In equation (4.11) and (4.12) only the downstream components were evaluated. These are the values of W_r which represent a sum of harmonic lee waves and constitute real wave motion.

5. Computations

De (1970) reported the occurrence of mountain waves in Assam and

... 9

neighbouring Burma-China hills during the winter season. The values of wavelength determined were compared with observed values determined from satellite cloud pictures, (De, (1971)).

Using the values of $\bar{U}$ and $\bar{T}$ from radiosonde and rawin observations of Gauhati, the values of $f(Z)$ were calculated at intervals of 0.25 km. The values of $f(Z)$ were then approximated by an exponential representation, i.e.,

$$f(Z) = f_0 e^{-\lambda Z}$$

and the values of f_0 and λ were determined. The solutions of the equation $J_m(\beta) = 0$ were obtained graphically, treating $J_m(\beta)$ as a function of m. From (4.5) we find,

$$m_n = \frac{2}{\lambda} Kn,$$

$$L = \frac{2\pi}{Kn}$$

where L is the wave length of the lee waves and m_n are the roots of $J_m(\beta) = 0$, and Kn is the wave number.

Using (4.10) the perturbation vertical velocities for different synoptic situations were computed for the Assam hill profile. The computations were carried out separately for the two ridges and graphically added. This is permissible because we are concerned here with a linear model. The following numerical values were used :

$a = 20.0$ km

$b_1 = 0.9$ km

... 10

b_2 = 0.7 km

d = 55.0 km

g = 10^{-2} km/sec^2

R = 29 x 10^{-5} km^{-2}/sec^2/deg

x = 1.4

ν^* = 10.0°C/km

6. Numerical solutions

If $W_1(x, Z)$ is resolved into its harmonic components by its Fourier transform

$$W(x, Z) = \int_0^\infty W'(Z, K)\, e^{ikx}\, dk, \qquad \ldots (6.1)$$

and substituted in equation (2.3) we find,

$$\frac{\partial^2 W'}{\partial Z^2} + (f(Z) - k^2)\, W' = 0 \qquad \ldots (6.2)$$

where,

$$W(x, Z) = \exp\left(\frac{g - R\nu}{2RT} Z\right) \int_0^\infty e^{ikx}\, W'(Z, k)\, dk$$

In this part we shall find the solutions of (6.2) by numerical integration with appropriate boundary conditions.

The lower boundary condition (4.7) provides,

$$W(x, 0) = \bar{U}(\xi)\, \frac{\partial}{\partial x}(\xi),$$

... 11

where,

$$\xi(x) = \frac{a^2 b_1}{a^2 + x^2} + \frac{a^2 b_2}{a^2 + (x-d)^2}$$

$$= ab_1 \int_0^\infty e^{-ak} e^{ikx}\, dk + ab_2 \int_0^\infty e^{-ak} e^{ik(x-d)}\, dk$$

The distance x is measured from the crest of the first ridge in the west-east direction.

At $Z = 0$, for a single ridge,

$$W'(0, k) = \bar{U}(0)\, e^{-ak}\, abik \qquad \ldots \qquad (6.3)$$

For the upper boundary condition, we note that the solution is indeterminate unless values of $f(Z)$ are specified at great heights. For numerical integration, we take actual values of $f(Z)$ at intervals of 0.25 km from the surface to a height H. Above H, we chose a constant value of $f(Z) = L$. The choice of L has only a small effect at low levels (Palm and Foldvik 1960, Corby and Sawyer 1958, Sawyer 1960).
We then have above $Z = H$,

$$W'(Z, k) = A \exp(i\nu_L Z) \quad \text{where,}$$
$$\nu_L^2 = L^2 - k^2$$
$$L^2 > k^2$$
$$= A \exp(-\nu'_L Z) \quad \text{where,}$$
$$\nu_L'^2 = k^2 - L^2$$
$$L^2 < k^2 \qquad (6.4)$$

and ν_L and ν'_L are positive numbers.

... 12

As pressure and vertical velocity are continuous functions of z at an interface, we assume w'_k and $\frac{\partial}{\partial z} w'_k$ are also continuous. Consequently, the upper boundary condition is,

$$\left.\begin{aligned} \frac{\partial}{\partial z} w'_k &= \nu_L w'_k \qquad K \leq L \\ &= \nu'_L w'_k \qquad K \geq L \\ &\text{at } Z = H \end{aligned}\right\} \tag{6.5}$$

To solve (6.2) with the above boundary conditions, we specify a function $\psi(z, k)$ which satisfies (6.2) and (6.5) at $Z = H$.

Consequently, $$\frac{\partial^2 \psi}{\partial z^2} + (f(z) - k^2)\,\psi = 0 \tag{6.6}$$

and

$$\left.\begin{aligned} &\frac{\partial \psi}{\partial z} = -i\nu_L \psi \quad \text{at } Z = H, \; K \leq L \\ &\qquad \text{Where, } \nu_L^2 = L^2 - K^2 \\ &\frac{\partial \psi}{\partial z} = -\nu'_L \psi \quad \text{at } Z = H, \; K \geq L \\ &\qquad \text{Where, } \nu_L'^2 = K^2 - L^2 \end{aligned}\right\} \tag{6.7}$$

We also assume for convenience,

$$\psi(H, K) = 1$$

Thus, w'_k is a simple multiple of ψ which will satisfy the lower boundary condition (6.3). Moreover,

$$w'_k = \bar{U}(0)\, a b i k \, \frac{\psi(Z, K)}{\psi(0, K)}\, e^{-ak} \tag{6.8}$$

The vertical velocity on account of both ridges is,

$$= Re\left\{\frac{\rho_0}{\rho_Z}\right\}^{1/2} \bar{U}(0) \left[\int_0^\infty a b_1 i k \, \frac{\psi(Z,K)}{\psi(0,K)}\, e^{-ak} e^{ikx}\, dk + \int_0^\infty a b_2 i k \, \frac{\psi(z,K)}{\psi(0,K)}\, e^{-ak} e^{ik(x-d)}\, dK\right] \tag{6.9}$$

where, we assume,

$$\exp\left(\frac{g - R_\nu}{2RT} z\right) \simeq \left(\frac{\rho_0}{\rho_z}\right)^{1/2}$$

We shall now discuss the quadrature of (6.9). Integration is difficult when the integrand has a singularity i.e. $\psi(0,k) = 0$

To remove the singularity, we subtract from the integrand a function which has a similar behaviour near the singular point. This function is,

$$\frac{\psi(z,K_\nu)}{\psi'(0,K_\nu)} \times \frac{\exp(-ak + ikx)\, abik}{(k - K_\nu)} \qquad (6.10)$$

where $K = K_\nu$ is a singular point.

Hence,

$$w(x,z) =$$

$$\mathrm{Re}\,\bar{U}(0)\left(\frac{\rho_0}{\rho_z}\right)^{1/2}\left[\int_0^\infty \left\{\frac{\psi(z,K)}{\psi(0,K)} - \sum_{\nu=1}^{N}\frac{\psi(z,K_\nu)}{\psi'(0,K_\nu)(K-K_\nu)}\right\} e^{-ak} e^{ikx}\, abik\, dk \qquad (6.11)\right.$$

$$\left. + \sum_{\nu=1}^{N}\frac{\psi(z,K_\nu)}{\psi'(0,K_\nu)}\int_0^\infty abik\,\frac{\exp(-ak+ikx)}{K-K_\nu}\,dk\right]$$

for a single ridge.

The integrand in the first integral of (6.11) is free from singularities. The second integral was evaluated by contour integration in the complex k-plane. The path of integration is shown in Fig.3. The path was chosen such that the singularity was confined to the upper quadrant only, thereby allowing only waves downstream of the barrier. Performing the integration and making the radii of indentations tend to zero and the radius of the circular arc tend to infinity, we get, for the second integral in (6.11),

$$\int_0^\infty abik\,\frac{\exp(-ak+ikx}{K-K_\nu}\,dk$$

$$= i(1+i)^2\int_0^\infty Kab\,\frac{\exp\left[\left\{-(a+x)+i(x-a)\right\}k\right]}{k(1+i)-K_\nu}\,dk$$

... 14

and $\int_0^\infty abik \frac{\exp(-ak-ikx)}{K-K_\nu} dk$

$= i(1+i)^2 \int_0^\infty Kab \frac{\exp\left[\left\{-(a-x)+i(x+a)\right\}K\right]dk}{K(1-i)-K_\nu}$, $x<0$

It is seen that a term of the form $2\pi i \exp(-ak_\nu + ik_\nu x)$ appears for, $x \geqslant 0$. This represents a lee wave. For simplicity we chose $f(Z) = L = 0$ above $Z = H$ (km). As indicated earlier, this choice has a very small effect on the flow at low levels. With this choice, is real, and the lee wave term represents a simple harmonic wave train extending infinitely downstream. The expression for vertical velocity is similarly divided into three parts x_1, x_2 and x_3 where,

$$x_1 = \int_0^\infty \left\{ \frac{\psi(Z,K)}{\psi(0,K)} - \sum_{\nu=1}^{N} \frac{\psi(Z,K_\nu)}{\psi'(0,K_\nu)(K-K_\nu)} \right\} abik \exp(-ak+ikx)dk \quad (6.12)$$

and for the region $x \geqslant 0$

$$x_2 = \sum_{\nu=1}^{N} \frac{\psi(Z,K_\nu)}{\psi'(0,K_\nu)} i(1+i)^2 \int_0^\infty \frac{Kab \exp\left[\left\{-(a+x)+i(x-a)\right\}K\right]dK}{(1+i)K-K_\nu} \quad (6.13a)$$

$$x_3 = 2\pi i \sum_{\nu=1}^{N} \frac{\psi(Z,K_\nu)}{\psi(0,K_\nu)(K-K_\nu)} \quad ik_\nu ab \exp(-ab_\nu + ik_\nu x) \quad (6.13b)$$

while for $x < 0$,

$$x_2 = \sum_{\nu=1}^{N} \frac{\psi(Z,K_\nu)}{\psi'(0,K_\nu)(K-K_\nu)} i(1-i)^2 \int_0^\infty Kab \frac{\exp\left[\left\{-(a-x)+i(x+a)\right\}K\right]dk}{(1+i)K-K_\nu} \quad (6.13c)$$

$x_3 = 0$.

The vertical velocity for a single ridge is given by,

$$w(x,Z) = \bar{U}(0)\left(\frac{\rho_0}{\rho Z}\right)^{1/2}\left[\text{Real part}\,(x_1+x_2+x_3)\right] \quad (6.14)$$

The numerical integration was carried out for 32 values of K for the range 0 to 5.0 km^{-1}. Equation (6.6) may be expressed in terms

$$\psi_{\nu-1} = -\psi_{\nu+1} + \left[2 - h^2\left(l_\nu^2 - K^2\right)\right]\psi_\nu$$

... 15

of finite difference by

$$\psi_{\nu-1} = -\psi_{\nu+1} + \left[2 - h^2(l_\nu^2 - k^2)\right]\psi_\nu \qquad (6.15)$$

where h is an interval of 0.25 km.

Integration starts from the upper Boundary where $\psi_N = 1$. We also put,

$$\left.\begin{aligned} \psi_{N-1} &= 1 - \frac{\nu_L^2 h^2}{2} - i\nu_L h \qquad K \leq L \\ &= 1 + \frac{\nu_L'^2 h^2}{2} + \nu_L' h \qquad K \geq L \end{aligned}\right\} \qquad (6.16)$$

Similarly, by differentiating (6.15) we get,

$$\psi'_{\nu-1} = -\psi_{\nu+1} + \left[2 + h^2(l_\nu^2 - k^2)\right]\psi'_\nu + 2kh^2\psi_\nu \qquad (6.17)$$

We put,

$$\left.\begin{aligned} \psi'_N &= 0 \\ \psi'_{N-1} &= kh^2 + \frac{ikh}{\nu_L} \qquad K \leq L \\ &= kh^2 + \frac{kh}{\nu_L'} \qquad K \geq L \end{aligned}\right\}$$

After evaluating the values of $\psi(Z, K)$ and $\psi'(Z, K)$ for all levels and for values of K ranging from 0 to 5.0 km^{-1}, we search for singularities or near singularities. We evaluate $\left[\frac{\psi(0,K)}{\psi(Z,K)}\right]^2$ for Z = 1 km at intervals of 0.05^{-1} from 0.1 km^{-1}, and at larger intervals upto 5 km^{-1}. The minima of $\left[\frac{\psi(0,K)}{\psi(Z,K)}\right]^2$ are used as starting points for an interative procedure to locate the zeros of the function

$$g = \frac{\psi(0,K)}{\psi(Z,K)}$$

The iterative recurrence relation is,

$$K_{s+1} = K_s - g_{K=K_s} \Big/ \left(\frac{\partial g}{\partial K}\right)_{K=K_s} \qquad (6.18)$$

These roots give the values corresponding to lee waves. Evaluation of the integrals in (6.12) was done by considering the integrand to be product of A(K) and exp (ikx), where A(K) is a slowly varying function of K. The integral between two successive pairs of ordinates K_1 and K_2 is,

... 16

$$\int_{K_1}^{K_2} A(k) \exp(ikx)\, dk$$
$$= \frac{2}{x} \left\{ \sin \frac{(K_2 - K_1)}{2} x \right\} \frac{A_1 + A_2}{2} \exp\left\{ ix \frac{(K_1 + K_2)}{2} \right\}$$
$$- \frac{i}{x} \left\{ \cos \frac{(K_2 - K_1)}{2} x - \frac{2}{x(K_2 - K_1)} \sin \frac{(K_2 - K_1)}{2} x \right\}$$
$$\times (A_2 - A_1) \exp\left\{ ix \frac{(K_2 + K_1)}{2} \right\} \qquad (6.19)$$

The displacement of stream lines was computed by using the relation between vertical velocity and stream function. We have

$$\bar{U}(z) \frac{\partial \xi}{\partial x}(x, z) = w(x, z) \qquad (6.20)$$

The values of ξ_N for each level were evaluated by the following marching scheme;

$$\frac{\bar{U}\left(-\xi_{N-1} + \xi_{N+1}\right)}{2h} = w_N$$

$$\xi_{N+1} = \xi_{N-1} + \frac{2h w_N}{U_N} \qquad (6.21)$$

The values of ξ thus obtained for $Z = 0$ were compared with the ground profile. The comparison showed that the values were in good agreement, and the error was less than 10% everywhere.

7. Results and Discussion

7.1 We computed the values of vertical velocity for seven cases analytically. We also computed the vertical velocity and displacement of stream lines for three situations by the numerical method. A summary of the results is presented in Table 1. The computations were made for larger wavelengths only (for wavelengths of the order of 20 km or more). It was

... 17

observed by computation that the smaller wavelengths did not produce appreciable vertical velocities; consequently, they are not presented in this paper. Details of each individual cases and diagrams are not being presented to save space.

7.2 In all cases, it was observed that the lapse rates at all levels were stable, often increasing with height. The lapse rate varied between 3 and 7° C/km. The wind speed was also found to increase with height often with increasing shear. The surface winds were of the order of 5 m sec^{-1}, reaching a value of the order of 50 m sec^{-1} at 12 km. The values of $f(Z)$ were a maximum at the surface and decreased rapidly near the ground layers smoothly with height. The surface values were of the order of 5 km^{-2}, which decreased to about .05 km^{-2} at a height of 10 km. The wind and temperature distribution and the distribution of $f(Z)$ with height, for a representative case (8.1.67), is shown in Fig.4(a) and 4(b). The variation of vertical velocity with height showed a sinusoidal pattern, varying from positive to negative values and again attaining positive values. The variation of vertical velocity with height for the above case is shown in Fig.5. The variation of vertical velocity downstream with distance is shown in Fig.6. It may be stated here that, depending upon the wave length, the superimposition of the two wave trains, which are due to two ridges having a fixed phase difference (due to d), may either intensify or dampen the waves beyond the second ridge.

7.3 Discussion of the numerical solution

We made computations by the numerical method on three occasions i.e. 8.1.67, 10.2.67 and 5.3.67. The complete vertical velocity field (X_1, X_2, and X_3) was computed for both ridges at different grid points in the

... 18

x - z plane. The vertical velocity pattern for 8.1.67 is shown in Fig.7. It was observed in all cases that vertical velocities far on the upstream side, i.e., beyond the first ridge at all levels were small; being less than 1 cm/sec. But, on the downstream side, the motion was sinusoidal in nature, i.e., the vertical velocity varied between positive and negative values over the same point at different heights. The maximum vertical velocity due to $X_1, X_2,$ and X_3 was of the order 1.4 m/sec. The vertical velocity pattern showed nodal lines sloping with height towards the upstream side.

7.4 The displacement of stream lines for the above case is shown in Fig. 8. For all three situations, the stream line displacements showed regular wave like oscillations to the lee of the barrier. Wave crests and troughs were found to tilt with height towards the upstream side. At large distances upstream, the displacements were very small and did not show any wave pattern. This is in agreement with the analytical computation of earlier workers.

8. Effects of narrow ridges

To demonstrate the effect of the size of an obstacle on the vertical velocity, we computed the vertical velocity for an arbitrary bell-shaped ridge (a = 10 km, b = 0.9 km). At all levels the computed vertical velocities were higher than those for the Assam hills, because the latter are much broader. The comparative values for a representative case (23.11.66) are shown in Fig. 9.

... 19

9. Conclusions

We may draw following conclusions from this study :-

(i) The airstream in Assam during the winter months has a favourable thermal stratification and wind shear to generate lee waves.

(ii) The vertical velocity associated with lee waves of 20-25 km wavelength varies from 10 cm sec^{-1} to 1.5 m sec^{-1} for the Assam hills, or any other obstacle of similar dimensions. For larger wave lengths (of the order of 70 km) the vertical velocities are higher and of the order of 4 m/sec. These values are in agreement with the computations of Sarker (1965).

(iii) The computations made for an arbitrary bell shaped obstacle (a = 10 km b = 0.9 km) suggest that lee waves observed in Assam could produce vertical velocities of the order of 2 m/sec on account of narrow isolated peaks.

(iv) The variation of vertical velocity is sinusoidal in nature, alternating between positive and negative values upto great heights.

(v) In the vertical velocity field the nodal lines tilt upstream. This is also true for ridges and troughs in the stream displacement field. This is in agreement with what we should expect in a fluid with thermal stratification.

(vi) The upward displacement of an airstream over the ridge reverses with height, sometimes at quite low levels.

10. Acknowledgements

The author wishes to express his thanks to Dr. R.P.Sarker, for suggesting the problem, for his guidance and many useful discussions. He is

... 20

thankful to the Director, Indian Institute of Tropical Meteorology, Poona, for providing necessary facilities for the work. Thanks are due to Miss A.G.Deodhar for assistance in computational work.

REFERENCES

Corby, G.A. and Sawyer, J.S.	1958	Q.J.R.M.S. Vol.84, pp.25-37
Das, P.K.	1964	I.J.M.G. Vol.15, No.4, pp.547-554
De, U.S.	1970	I.J.M.G. Vol.21,No.4, pp.637-642
De, U.S.	1971	National Symposium on Satellite Meteorology, India (I.J.M.G., Vol.22, No.3, pp.361-364).
Doos, BOR	1958	Tech.Report No.13, Contract No. Nour 600 (00) Florida State University, Florida.
Doos, BOR	1961	Tellus, Vol.13, p.305
Doos, BOR	1962	Tellus, Vol.14, p.301
Foldvik, A.	1962	Q.J.R.M.S., Vol.88, p.271
Foldvik, A. and Palm, E.	1957	Inst.Weath. and Climate Res., Oslo, Report No.7
Foldvik, A. and Palm, E.	1959	Ibid, Report No.4
Palm, E. and Foldvik, A.	1960	Geof.Publ. 21, 6, Oslo
Kelvin, Lord	1886	Phil Mag.5, 22 pp.353, 445, 517
Palm, E.	1958	Geof. Publ. 20, 3, Oslo
Sarker, R.P.	1965	I.J.M.G., Vol.16, No.4, pp.565-584
Sarker, R.P.	1967	Mon.Weath.Rev., Vol.94, No.9
Sawyer, J.S.	1960	Q.J.R.M.S., Vol.86, p.326
Scorer, R.S.	1949	Q.J.R.M.S., Vol.75, p.41

--oOo--

IITM/SGG/1972. (Received September 5, 1972; revised October 7, 1972)

TABLE - 1.

Sr. No.	Date	Computed values L (KM)					Vertical velocity Maximum (Height)			Remarks
1	23.11.66	78.1	20.5	11.3	7.4	5.3	4.3	m/sec	(12KM)	Analytically computed corresponding to L = 78.1 KM
							20.30	cm/sec	(12 KM)	Corresponding to L = 20.5 KM.
2	1.12.66	19.4	7.14				13.20	"	(6 KM)	Corresponding to L = 19.4 KM.
3	8.1.67	20.2	7.3				19.70	"	(7 KM)	Corresponding to L = 20.2 KM.
	8.1.67	25.3	7.1				-85.60	"	(8 KM)	Numerically computed for wave-part only L = 25.3 KM.
4	9.1.67	18.7	7.9				13.50	"	(6 KM)	Analytically computed corresponding to L = 20.2 KM.
5	14.2.67	17.4	6.3				6.15	"	(5 KM)	Corresponding to L = 17.4 KM.
6	10.2.67	23.1	8.9				31.02	"	(8 kM)	Numerically computed for Wave-part only L = 23.1 KM.
7	5.3.67	23.1	8.3				+22.40	"	(6 KM)	Numerically computed for wave-part only L = 23.1 KM.

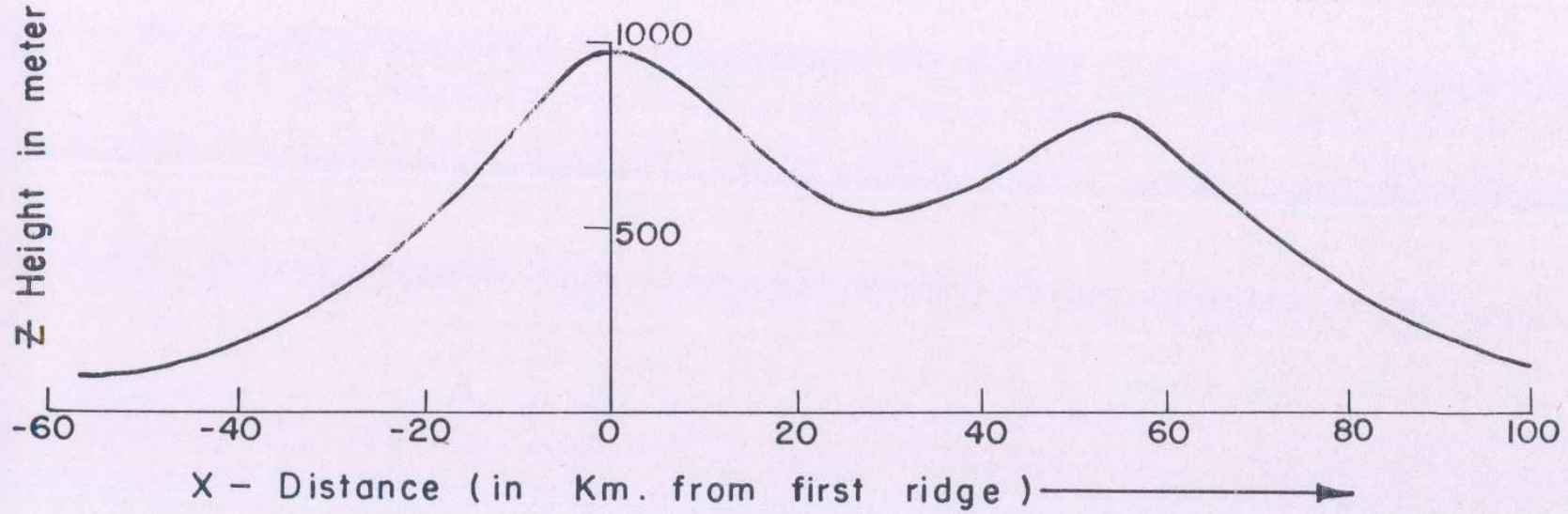
Z Height in meter
1000
500
-60
-40
-20
0
20
40
60
80
100
X – Distance (in Km. from first ridge)

FIG. 1.

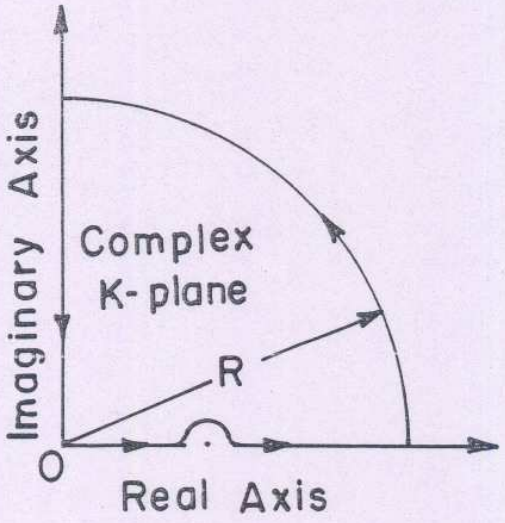

Path of contour integration

Fig: 2

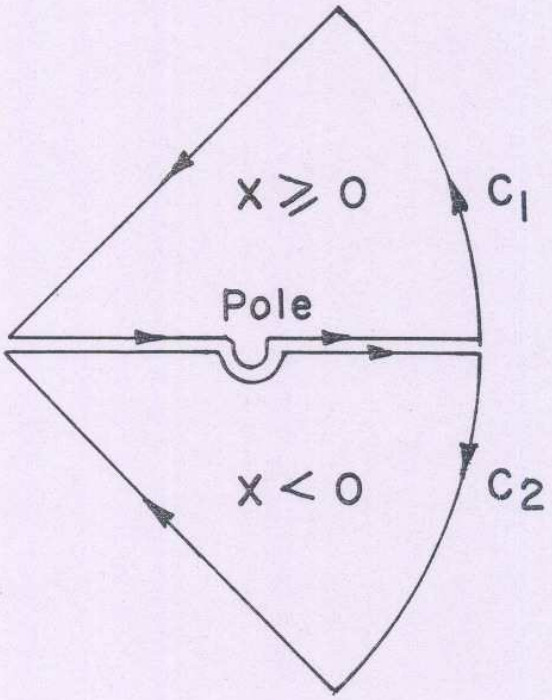

Path of contour integration

Fig· 3

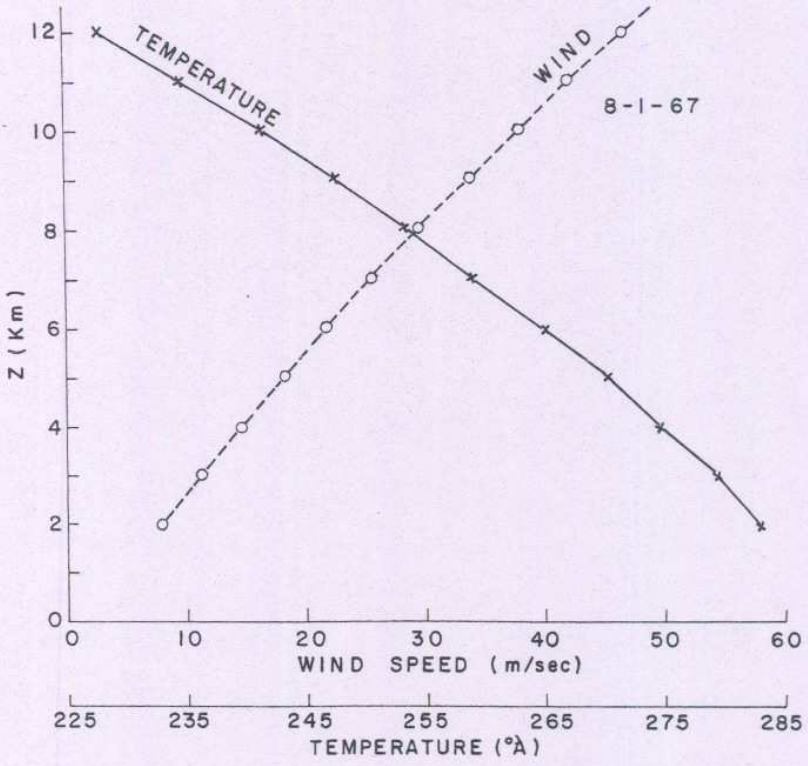
TEMPERATURE
WIND
8-1-67
Z (Km)
WIND SPEED (m/sec)
TEMPERATURE (°A)

FIG. 4(a)

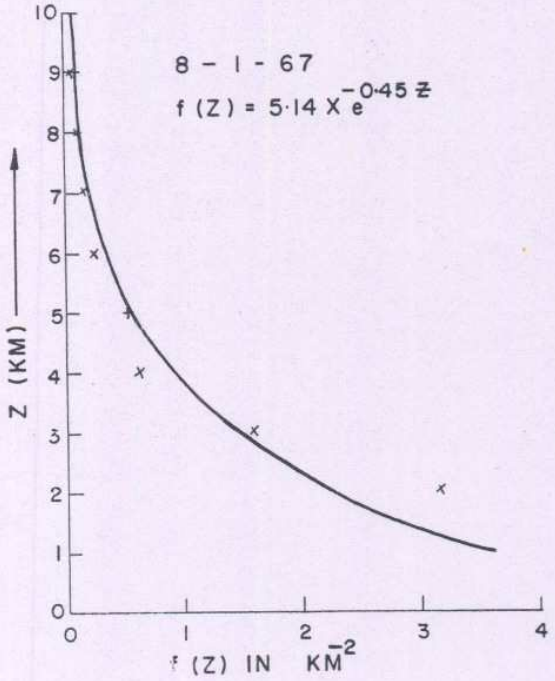
8 - 1 - 67
f (Z) = 5·14 X e^-0·45 Z
Z (KM)
f (Z) IN KM^-2

FIG. 4 (b)

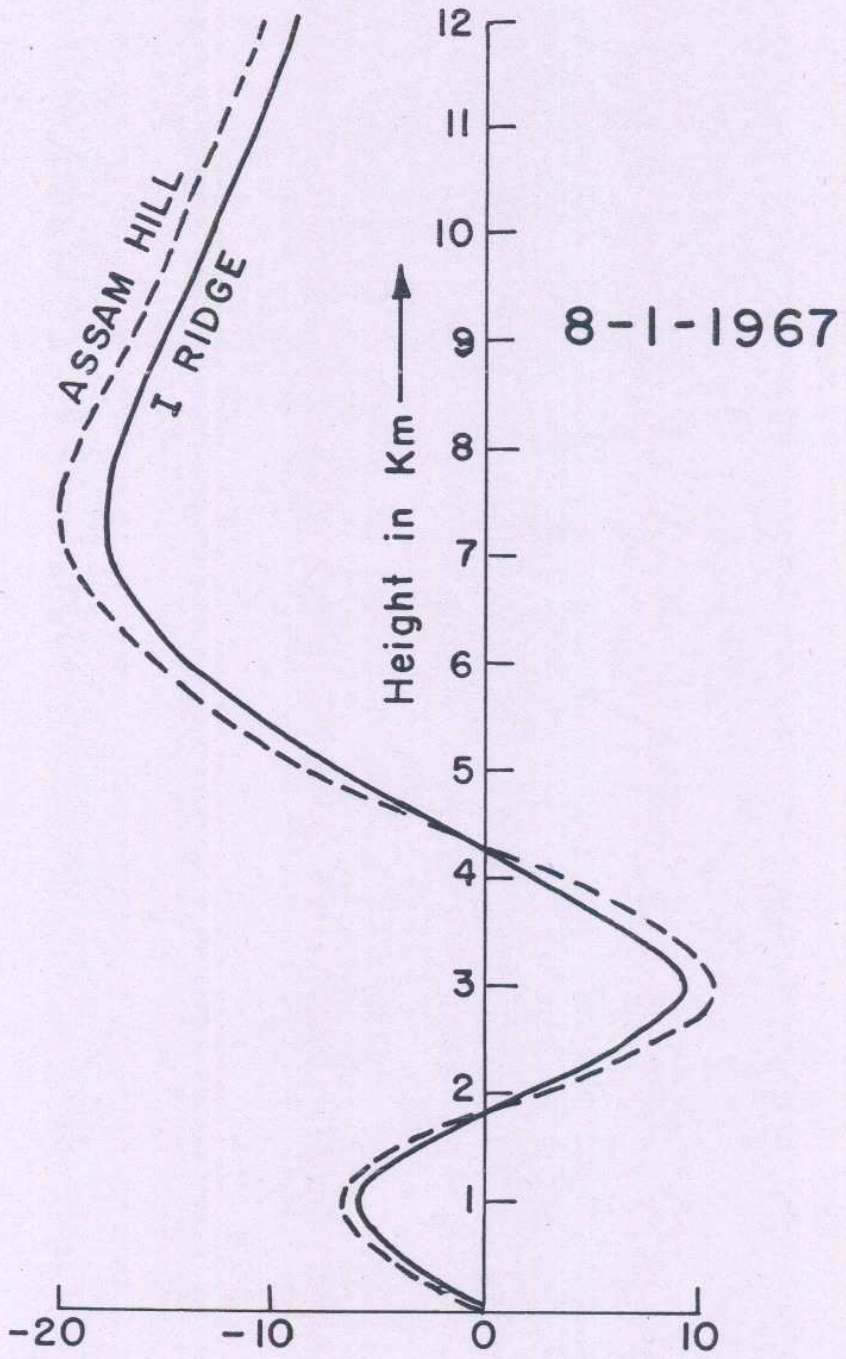
ASSAM HILL
I RIDGE
8-1-1967
Height in Km
12
11
10
9
8
7
6
5
4
3
2
1
-20
-10
0
10
Amplitude of vertical velocity
in cm/sec

FIG. 5.

8 - 1 - 67

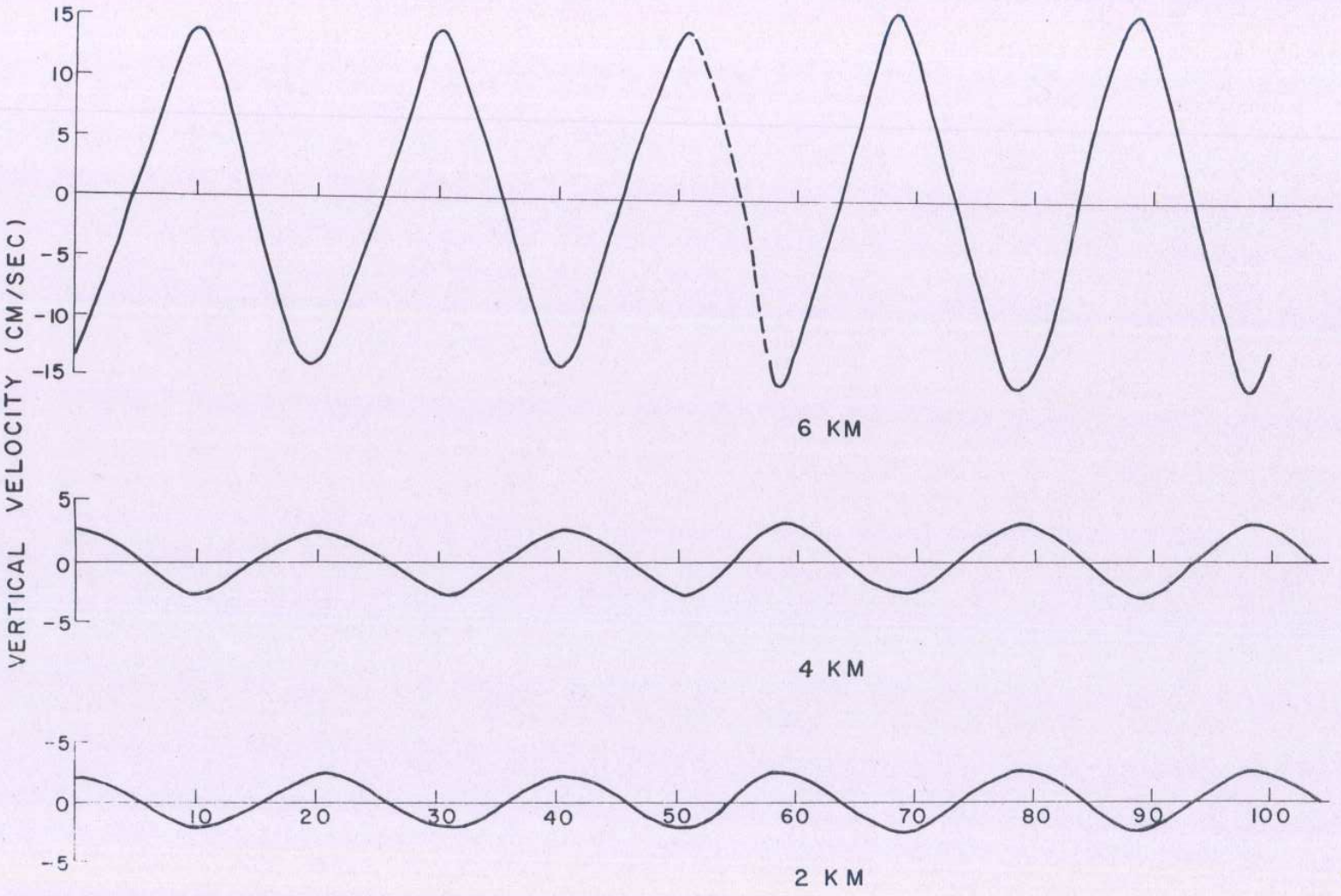
VERTICAL VELOCITY (CM/SEC)
15
10
5
0
-5
-10
-15
6 KM
5
0
-5
4 KM
-5
0
-5
10
20
30
40
50
60
70
80
90
100
2 KM
DISTANCE IN KM
(From first ridge)

FIG. 6

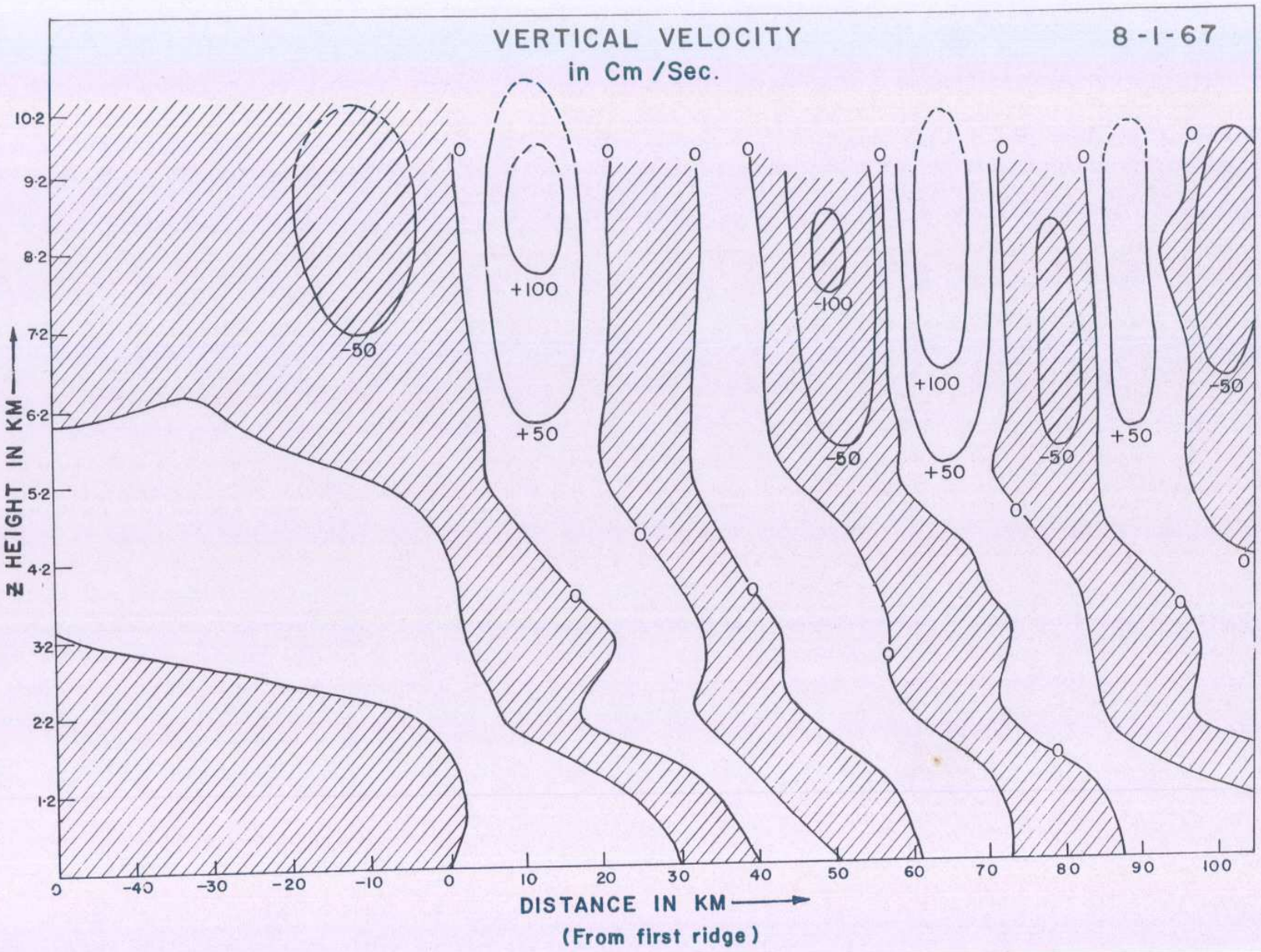
VERTICAL VELOCITY
in Cm /Sec.
8-1-67
Z HEIGHT IN KM
10·2
9·2
8·2
7·2
6·2
5·2
4·2
3·2
2·2
1·2
+100
-50
+50
-100
-50
+100
+50
-50
+50
-50
0
-40
-30
-20
-10
0
10
20
30
40
50
60
70
80
90
100
DISTANCE IN KM
(From first ridge)

FIG· No. 7

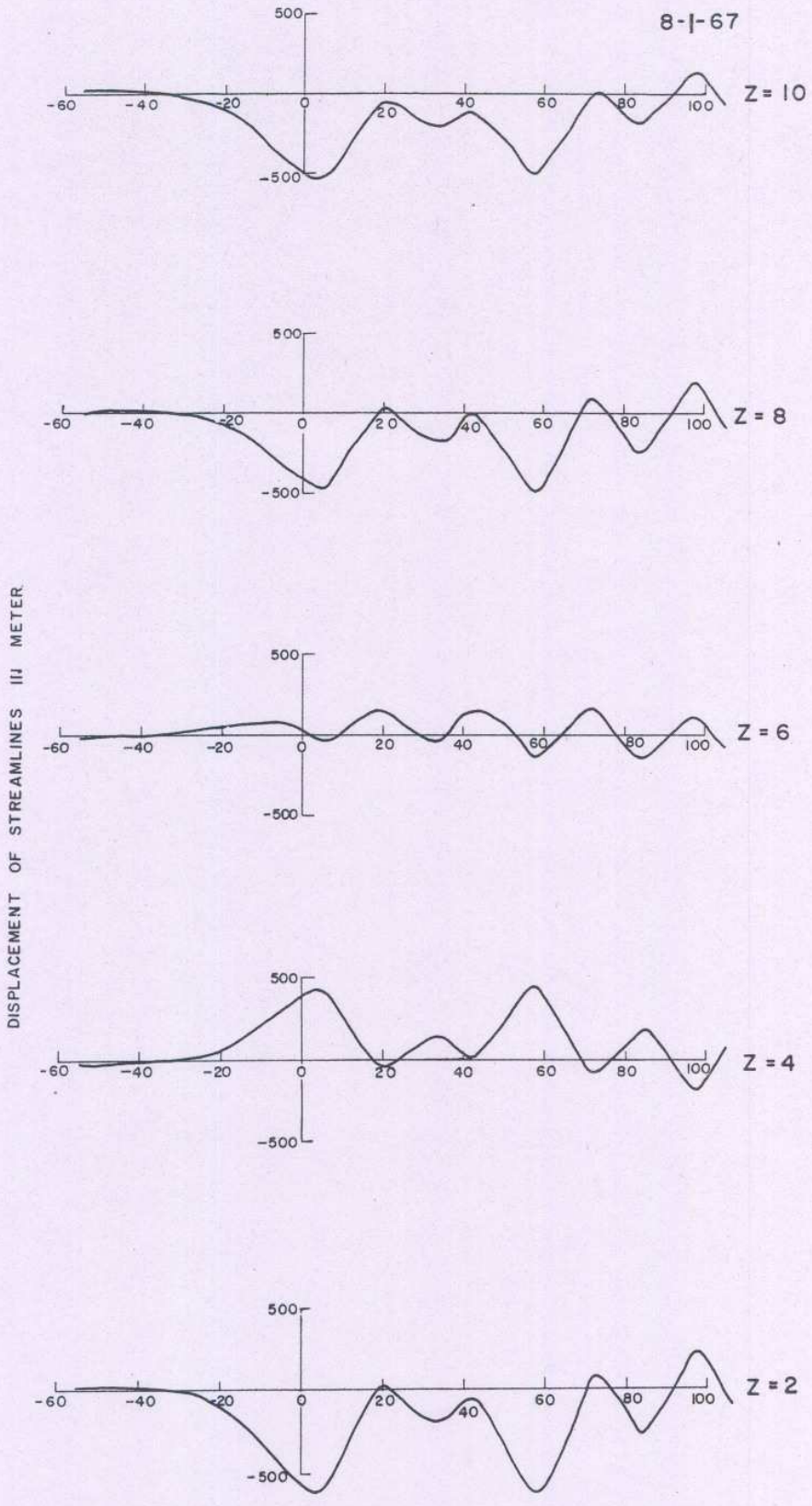
8-1-67
Z = 10
Z = 8
Z = 6
Z = 4
Z = 2
500
-500
-60
-40
-20
0
20
40
60
80
100
DISPLACEMENT OF STREAMLINES IN METER
DISTANCE IN KM
(from first ridge)

FIG. 8

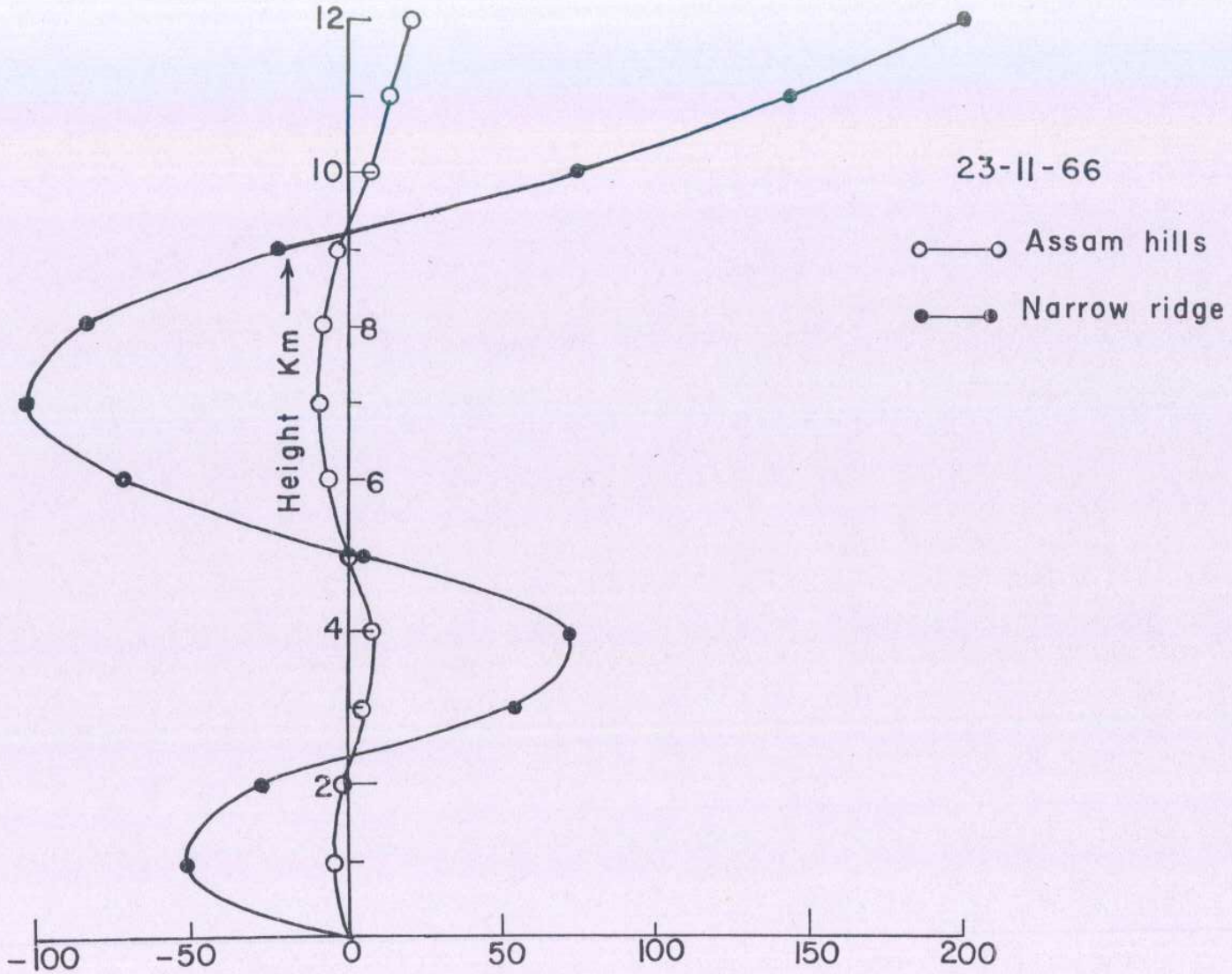
12
10
8
6
4
2
Height Km
23-11-66
Assam hills
Narrow ridge
-100
-50
0
50
100
150
200
VERTICAL VELOCITY Cm/Sec

Fig. 9

E R R A T A

Page 1 Line 6 delete SW

Page 5 Equation (4.2) replace W by W_o

Page 5 Equation (4.3) replace W by W_o

Page 5 Equation (4.5) replace W by W_o

Page 13 Equation in the last line

add $+2\pi i\, ikr\, ab\, \exp(-akr + ikr\, x),\ x \geq o$

Page 14 R.H.S. of equation on at the top of the page change

$(1+i)^2$ to $(1-i)^2$

Page 14 Equation (6.13 (a)) read as,

$$x_2 = \sum_{r=1}^{N} \frac{\psi(z, kr)}{\psi'(o, kr)}\, i\,(1+i)^2 \times$$

$$\times \int_0^{\infty} kab\, \exp\left[\{-(a+x) + i(x-a)\}k\right] dk$$

$$(1+i)k - kr$$

Page 14 Equation (6.13 (b)) read as

$$x_3 = 2\pi i \sum_{r=1}^{N} \frac{\psi(z, kr)}{\psi'(o, kr)}\, ikr\, ab\, \exp(-akr + ikr\, x)$$

Page 14 Equation (6.13 (c)) read as

$$x_2 = \sum_{r=1}^{N} \frac{\psi(z, kr)}{\psi'(o, kr)} \cdot i\,(1-i)^2 \times \int_0^{\infty} kab\, \exp\left[\{-(a-x) + i(x+a)\}k\right] dk$$

$$(1+i)k - kr$$

Page 15 In Equation (6.15) & (6.17)

replace l_r^2 by f_r